Chemical Science

EDGE ARTICLE

View Article Online
View Journal | View Issue

Cite this: *Chem. Sci.*, 2019, **10**, 9326

All publication charges for this article have been paid for by the Royal Society of Chemistry

Received 21st June 2019
Accepted 19th August 2019

DOI: 10.1039/c9sc03076j

rsc.li/chemical-science

Electrochemical C–H bond activation *via* cationic iridium hydride pincer complexes†

Brian M. Lindley, ‡[a] Andrew G. Walden,‡[ab] Ann Marie Brasacchio,[ac] Andrea Casuras,[d] Nicholas Lease,[d] Chun-Hsing Chen,[a] Alan S. Goldman [d] and Alexander J. M. Miller *[a]

A C–H bond activation strategy based on electrochemical activation of a metal hydride is introduced. Electrochemical oxidation of (^{tBu_4}PCP)IrH$_4$ (^{tBu_4}PCP is [1,3-(^{t}Bu$_2$PCH$_2$)-C$_6$H$_3$]$^-$) in the presence of pyridine derivatives generates cationic Ir hydride complexes of the type [(^{tBu_4}PCP)IrH(L)]$^+$ (where L = pyridine, 2,6-lutidine, or 2-phenylpyridine). Facile deprotonation of [(^{tBu_4}PCP)IrH(2,6-lutidine)]$^+$ with the phosphazene base *tert*-butylimino-tris(pyrrolidino)phosphorane, ^{t}BuP$_1$(pyrr), results in selective C–H activation of 1,2-difluorobenzene (1,2-DFB) solvent to generate (^{tBu_4}PCP)Ir(H)(2,3-C$_6$F$_2$H$_3$). The overall electrochemical C–H activation reaction proceeds at room temperature without need for chemical activation by a sacrificial alkene hydrogen acceptor. This rare example of undirected electrochemical C–H activation holds promise for the development of future catalytic processes.

Introduction

The activation of C–H bonds has become one of the most powerful tools in chemical synthesis.[1,2] Among the diverse mechanistic pathways available to transition metal complexes for C–H bond activation, C–H oxidative addition at a low-valent metal center is perhaps the most prominent. This reaction underpins thermal C–H functionalization by iridium pincer complexes that have proven to be especially prolific catalysts.[3] The archetypal dihydride complex (^{tBu_4}PCP)Ir(H)$_2$ and its H$_2$ adduct (^{tBu_4}PCP)IrH$_4$ (**1**, Scheme 1)[4] catalyze an array of reactions based on alkane dehydrogenation, as well as C–O and C–F activation reactions that are initiated by sp^3 C–H bond activation.[3] Efficient dehydrogenation catalysis requires a sacrificial alkene (*e.g.* *tert*-butylethylene, TBE) to generate a three-coordinate iridium(I) intermediate (^{tBu_4}PCP)Ir that rapidly activates hydrocarbon C–H bonds. Catalyst activation by the sacrificial alkene is the rate-determining step in some (^{tBu_4}PCP)Ir-catalyzed C–H functionalization systems.[3,5]

Electrochemical oxidation of pincer iridium hydride complexes (Scheme 1, green) represents a possible alternative to the use of sacrificial alkene hydrogen acceptor reagents. Sequential removal of H$^+$ and e$^-$ equivalents would result in a (perhaps counterintuitive) change in formal oxidation state from Ir(III) to Ir(I) upon oxidation, generating the key three-coordinate intermediate (^{tBu_4}PCP)Ir.

Electrochemical C–H functionalization has recently enabled impressive advances in synthetic organic chemistry, either *via* direct electrochemical activation of organic substrates,[6,7] or *via* electrochemical regeneration of organometallic complexes to close a catalytic cycle.[8–10] The latter processes are notably limited to substrates with directing groups that pre-organize and accelerate the C–H bond activation. To our knowledge,

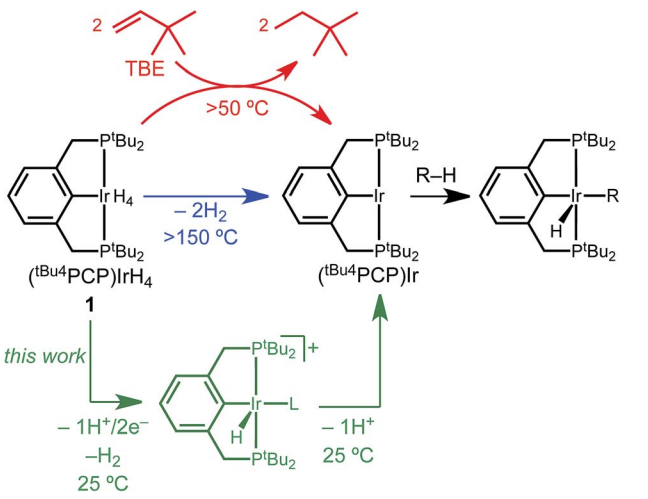

Scheme 1 Comparison of thermal and electrochemical C–H activation by pincer iridium complexes.

[a]*Department of Chemistry, University of North Carolina at Chapel Hill, Chapel Hill, North Carolina 27599-3290, USA. E-mail: ajmm@email.unc.edu*

[b]*Oglethorpe University, Atlanta, Georgia 30319, USA*

[c]*High Point University, High Point, NC 27262, USA*

[d]*Rutgers, The State University of New Jersey, New Brunswick, New Jersey 08903, USA*

† Electronic supplementary information (ESI) available. CCDC 1935784, 1935785 and 1935786. For ESI and crystallographic data in CIF or other electronic format see DOI: 10.1039/c9sc03076j

‡ These co-authors contributed equally.

there are no conclusive examples of electrocatalytic C–H bond activation of sp^2 or sp^3 C–H bonds lacking directing groups, and no examples of electrochemically driven intermolecular C–H activation with the versatile family of (PCP)Ir-based complexes.[11]

We present a detailed investigation of the electrochemical C–H bond activation of 1,2-difluorobenzene by tetrahydride **1**. In demonstrating the elementary steps of Scheme 1, a series of stabilized cationic iridium hydride complexes was isolated and characterized and found to cleanly activate the arene upon deprotonation. The overall reaction utilizes electrochemistry to achieve C–H bond activation of a directing-group-free substrate at room temperature, without a sacrificial chemical hydrogen acceptor.

Results and discussion

Electrochemical synthesis of a cationic iridium hydride

Several factors guided the selection of conditions that would be suitable for electrochemical C–H bond activation by pincer iridium hydrides. First, we recognized that the three-coordinate intermediate ($^{t\mathrm{Bu}_4}$PCP)Ir reacts with the C–H bonds of most common solvents, leading us to consider conditions of large substrate excess (or substrate as solvent). A second concern was the ability of the substrate-solvent to dissolve a supporting electrolyte and present a suitable electrochemical potential window, given that many potential substrates are non-polar and thus unsuitable for preparative scale electrochemistry. With these constraints in mind, we selected 1,2-difluorobenzene (1,2-DFB) as an arene substrate[12] without directing groups that is suitably polar to dissolve commonly employed electrolytes such as $[^n\mathrm{Bu}_4\mathrm{N}][\mathrm{PF}_6]$ and is stable over a wide potential window, especially in the oxidative direction.[13–15] The tetrahydride **1** was the focus of investigations, based on excellent stability observed in control experiments (whereas the dihydride underwent partial decomposition in polar solvents). Based on our prior observation that oxidation of ($^{t\mathrm{Bu}_4}$PCP)Ir(H)$_n$ (n = 2, 4) in THF leads to decomposition in the absence of a stabilizing ligand,[16] we hypothesized that key cationic intermediates might need to be stabilized. Neutral ligands that provide good σ donation and weak π back-donation were targeted as candidates to stabilize cationic Ir(III) but readily dissociate upon deprotonation to neutral Ir(I).

We initiated our studies by exploring whether cationic complexes stabilized by pyridine and its analogues could be accessed electrochemically and serve as intermediates in the C–H bond activation of 1,2-DFB. It has been recognized previously that oxidation can greatly increase the acidity of metal hydrides,[17] so we anticipated pyridine could act as a base and a ligand. Pyridine itself was found to react with **1** (see ESI Section 3†), however, so we turned to the bulkier congener 2,6-lutidine.

Cyclic voltammetry (CV) of **1** in 1,2-DFB containing 0.2 M $[^n\mathrm{Bu}_4\mathrm{N}][\mathrm{PF}_6]$ electrolyte and decamethylferrocene as an internal standard revealed an irreversible oxidation at approximately 0.35 V *vs.* $Cp_2Fe^{+/0}$ at 100 mV s^{-1}. The iridium complex is significantly easier to oxidize than 2,6-lutidine, which is oxidized beyond 0.7 V *vs.* $Cp_2Fe^{+/0}$.

The CV data guided the choice of conditions for preparative electrochemical synthesis. The tetrahydride **1** and 11 equiv. 2,6-lutidine were subjected to controlled potential electrolysis (CPE) at 0.90 V *vs.* $Ag^{+/0}$ (approx. 0.4 V *vs.* $Cp_2Fe^{+/0}$) in 1,2-DFB with $[^n\mathrm{Bu}_4\mathrm{N}][\mathrm{PF}_6]$ electrolyte. During the 1.5 h electrolysis, charge equivalent to 2.1e$^-$ per Ir was passed and a color change from pale to dark yellow was observed. Analysis by ^{1}H NMR spectroscopy confirmed formation of a new species assigned as the target cationic 2,6-lutidine (lut) adduct, $[(^{t\mathrm{Bu}_4}\mathrm{PCP})\mathrm{Ir}(\mathrm{H})(\mathrm{lut})]^+$ in 83% ^{1}H NMR yield based on the mesitylene internal standard (Scheme 2).

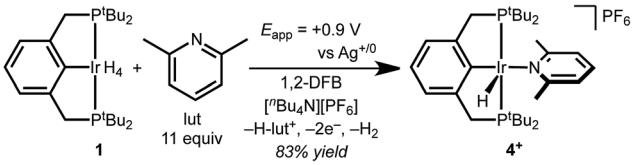

Scheme 2 Electrosynthesis of cationic iridium hydride 4^+.

Independent synthesis and characterization of cationic iridium hydride complexes

An independent synthetic route to cationic hydrido pyridine complexes was designed based on halide abstraction from ($^{t\mathrm{Bu}_4}$PCP)Ir(H)(Cl) (**2**). As shown in Scheme 3, equimolar mixtures of **2** and substituted pyridines were treated with $NaBAr^F_4$ (Ar^F = 3,5-bis(trifluoromethyl)phenyl) in CH_2Cl_2. This route was used to obtain pyridine complex $[(^{t\mathrm{Bu}_4}\mathrm{PCP})\mathrm{Ir}(\mathrm{H})(\mathrm{py})][BAr^F_4]$ ($\mathbf{3}^+$), 2,6-lutidine complex $[(^{t\mathrm{Bu}_4}\mathrm{PCP})\mathrm{Ir}(\mathrm{H})(\mathrm{lut})][BAr^F_4]$ ($\mathbf{4}^+$), and 2-phenylpyridine (2-Phpy) complex $[(^{t\mathrm{Bu}_4}\mathrm{PCP})\mathrm{Ir}(\mathrm{H})(2\text{-Phpy})][BAr^F_4]$ ($\mathbf{5}^+$). For pyridine, stoichiometric control is important to prevent further binding of pyridine to $\mathbf{3}^+$ (see ESI Section 3†), while further binding of lut and 2-Phpy to $\mathbf{4}^+$ and $\mathbf{5}^+$ was not observed.

Cationic hydrides supported by the archetypal $^{t\mathrm{Bu}_4}$PCP ligand are surprisingly rare,[18,19] so these species were fully characterized. Multinuclear NMR spectra of $\mathbf{3}^+$ are consistent with a square pyramidal geometry with an apical hydride ligand, on the basis of the highly upfield-shifted ^{1}H NMR signal for the hydride at −45.4 ppm.[18] Complexes $\mathbf{4}^+$ (−31.4 ppm) and $\mathbf{5}^+$ (−20.1 ppm) feature hydride ^{1}H NMR signals that are shifted downfield relative to that of $\mathbf{3}^+$ (−45.4 ppm). Hydride chemical shifts in octahedral Ir(III) complexes reflect the presence and

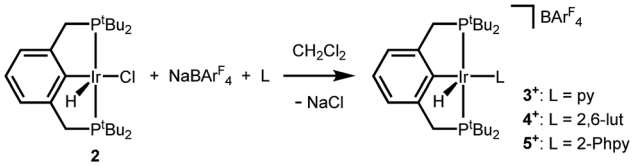

Scheme 3 Synthesis of cationic hydride complexes.

nature of ligands *trans* to the hydride donor,[20,21] so the large span of chemical shifts indicated unexpectedly significant changes in geometry (particularly given that the hydride of 3^+ is assigned to be *trans* to a vacant coordination site).

Single crystals of complexes 3^+, 4^+, and 5^+ were obtained, enabling a comparative XRD study evaluating the molecular geometry with each pyridine ligand in the solid state (Fig. 1). Cationic hydrido pyridine complex 3^+ features a square pyramidal structure, with a 179.8° angle between the aryl backbone C, central Ir, and the pyridine N, similar to the C–Ir–C(O) angle in $[(^{tBu_4}PCP)Ir(H)(CO)]^+$.[18] The same C–Ir–N angle in the 2,6-lutidine complex 4^+ is 174.5°, while in the structure of 2-phenylpyridine complex 5^+ the pyridyl nitrogen is canted dramatically, nearly reaching a position *cis* to the phenyl backbone (C–Ir–N 99°). The phenyl ring of 2-Phpy is held proximate to the site *trans* to the phenyl backbone in 5^+. DFT geometry optimization studies (see ESI Section 7†) on the series of complexes shows a widening H–Ir–N angle from 90.6° for 3^+ to 112.6° for 4^+ and 175.9° for 5^+. This perturbation from a *cis* orientation of pyridine and hydride donors to a *trans* orientation is fully consistent with the observed downfield hydride ^{1}H NMR chemical shifts. The computed structure of 4^+ is more dramatically bent than observed in the experimental XRD study, with evidence from DFT for a lutidine methyl C–H agostic interaction *trans* to the hydride (Ir–C 2.95 Å).

The proximity of the 2-Phpy phenyl ring to the Ir center in 5^+ (Ir–C35 2.565(6) Å) is consistent with an agostic interaction involving an aromatic proton on the phenyl substituent of 2-Phpy. While no upfield resonances of 5^+ indicative of an agostic interaction were observed by ^{1}H NMR spectroscopy at room temperature in CD_2Cl_2, cooling the sample to −20 °C resulted in sharper, more resolved aromatic resonances and the appearance of a new singlet at 4.01 ppm coupled to an aromatic carbon ($\delta_{^{13}C} = 97.1$, $^1J_{CH} = 125$ Hz). The upfield shifts in both the ^{1}H and ^{13}C resonances, as well as the substantially reduced $^1J_{CH}$ (typically 150–170 for aromatic C–H), are hallmarks of a C–H agostic interaction.[22]

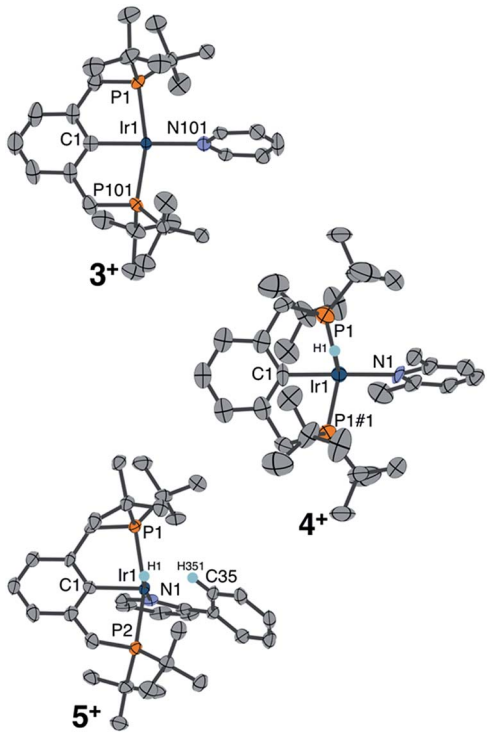

Fig. 1 Structural representation of 3^+, 4^+, and 5^+ from XRD with ellipsoids rendered at 50% probability. Most hydrogen atoms and all BAr^F_4 counter ions omitted for clarity. Hydride hydrogen atom of 3^+ was not located in the difference map. Selected bond distances (Å) and angles (°), 3^+: Ir1–P1 2.324(2), Ir1–P101 2.329(5), Ir1–N101 2.135(7), P1–Ir1–P1#1 163.6(1), C1–Ir1–N1 179.99(4); 4^+: Ir1–P1 2.345(2), Ir1–N1 2.131(9), Ir1–C1 2.008(11), P1–Ir1–P1#1 157.11(15), C1–Ir1–N1 174.5(5); 5^+: Ir1–P1 2.365(2), Ir1–P2 2.345(2), Ir1–N1 2.192(5), Ir1–C1 2.038(6), P1–Ir1–P2 158.02(6), C1–Ir1–N1 98.7(2).

Deprotonation of cationic iridium hydride complexes

With well-defined and electrochemically accessible cationic hydrides in hand, base-promoted C–H bond activation was targeted. Treating 2,6-lutidine complex 4^+ with 1 equiv. ^{t}BuP$_1$(pyrr) in 1,2-DFB resulted in full conversion within minutes at room temperature. Two sets of product signals with upfield hydride resonances indicative of five-coordinate Ir(III) complexes (−43.2, −46.3 ppm) are observed by ^{1}H NMR spectroscopy. New ^{1}H and ^{19}F resonances confirm the presence of a fluoroaryl group bound to iridium.[12] The combined spectroscopic data are consistent with clean conversion to $(^{tBu_4}PCP)Ir(H)(2,3\text{-}C_6F_2H_3)$ as a mixture of rotamers, **6a** and **6b** (Scheme 4). This structure was confirmed by addition of CO to produce the known complex $(^{tBu_4}PCP)Ir(H)(CO)(2,3\text{-}C_6F_2H_3)$.[23] The high regioselectivity, with exclusive C–H bond activation at the 3-position, is expected based on the *ortho*-fluorine stabilizing effect.[24–26]

While the agostic interaction of 5^+ seemed likely to bias C–H activation reactivity towards cyclometallation, deprotonation of 5^+ in 2-phenylpyridine solutions led to a mixture of several species at room temperature, only converging to the expected *ortho*-metallated phenylpyridine complexes upon heating (indicating that C–H addition occurs without prior pyridine coordination, as noted previously).[12,27–29] Further studies focused on the well-defined reactivity of 4^+ in 1,2-DFB.

Electrochemical C–H activation of 1,2-difluorobenzene

Having successfully demonstrated both key steps in the proposed C–H bond activation scheme, we next attempted

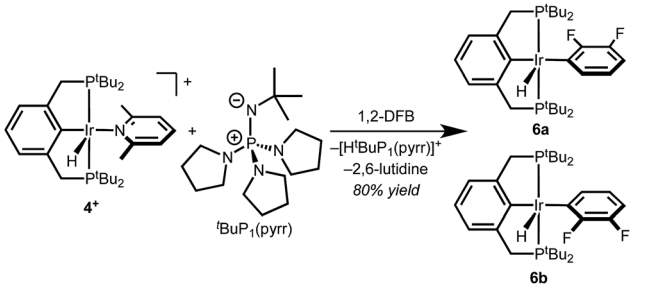

Scheme 4 C–H activation of 1,2-DFB by deprotonation of 4^+.

a one-pot electrochemical C–H activation of 1,2-DFB starting from ($^{t\mathrm{Bu}_4}$PCP)IrH_4, 20 equiv. lut, and 5 equiv. ^{t}BuP_1(pyrr). Oxidation by CPE resulted in a color change from pale orange to dark orange-red, and passage of current amounting to 2.7e$^-$ per Ir. Analysis of the product mixture by ^{1}H NMR spectroscopy showed that **1** indeed provided **6a** and **6b**, but with limited conversion (19% yield, Scheme 5). The reaction proceeds in higher yield (30%) when the 2,6-lutidine is left out of the reaction. The formation of the desired product is a promising indication of the viability of this electrochemical C–H activation strategy.

We hypothesized that incomplete conversion of **1** in the electrochemical process was due to complications arising from direct oxidation of the base, ^{t}BuP_1(pyrr). Indeed, ^{t}BuP_1(pyrr) is more easily oxidized than **1** (Fig. S33 in the ESI†) and we suspect that the oxidized ^{t}BuP_1(pyrr) may lead to electrode fouling or other side reactions.

To circumvent direct oxidation of ^{t}BuP_1(pyrr), a one-pot procedure was carried out. Electrochemical generation of $\mathbf{4}^+$ was followed immediately by addition of ^{t}BuP_1(pyrr), producing **6a** and **6b** in a significantly improved yield of 61%.

Comparison to sacrificial olefin-mediated process

To compare electrochemical and thermal C–H activation processes, the reactivity of ($^{t\mathrm{Bu}_4}$PCP)IrH_4 in 1,2-DFB with the prototypical hydrogen acceptor *tert*-butylethylene (TBE) was evaluated. Allowing ($^{t\mathrm{Bu}_4}$PCP)IrH_4 to react with 2 equiv. TBE in 1,2-DFB led to no observed reaction after 24 hours at 20 °C. Heating the mixture at 50 °C for 17 h resulted in full conversion to a mixture of products, of which 79% were C–H activation products of 1,2-DFB in a 1.6 : 1 ratio (**6a** : **6b**).

The thermal and electrochemical arene activation reactivity are notably distinct. The traditional thermal approach requires a sacrificial alkene (TBE) as a chemical hydrogen acceptor, producing an equivalent of 2,2-dimethylbutane as a byproduct. Given that both the chemical and electrochemical reactions are proposed to proceed through the same ($^{t\mathrm{Bu}_4}$PCP)Ir intermediate, the elevated temperatures required by the thermal C–H bond activation reaction are consistent with a rate-determining reaction with TBE, in accord with previous studies.[5] The new electrochemical approach, in contrast, does not require an olefinic sacrificial hydrogen acceptor. The electrochemical method described here does require a chemical additive in the form of a phosphazene base. In an envisioned electrochemical application, the protonated base would migrate to the cathode and supply protons for H_2 evolution, regenerating the free base. Furthermore, the low barrier to electrochemical activation to reach the ($^{t\mathrm{Bu}_4}$PCP)Ir intermediate allows the reaction to proceed at room temperature.

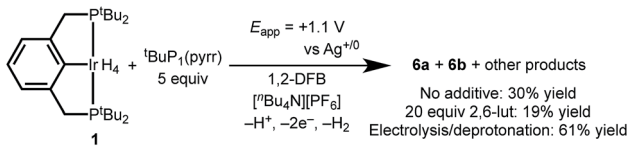

Scheme 5 Electrochemical C–H activation of 1,2-DFB by **1**.

Conclusions

The need for alkene hydrogen acceptors has been a major limitation in (PCP)Ir-catalyzed C–H functionalization reactions. The electrochemical C–H activation conditions reported here lift the requirement for sacrificial hydrogen acceptor reagents. Furthermore, the electrochemical reaction proceeds at room temperature, whereas even the acceptor-driven reaction must be heated. Cationic iridium hydride complexes are likely intermediates in the electrochemical C–H bond activation pathway. Three such species were isolated and characterized, displaying a rich structural diversity that may be attributed to agostic interactions.

This work illuminates some areas where modified catalysts or conditions could be beneficial. First, a solvent that can support electrochemical studies while withstanding reaction with the Ir complex is needed. Second, the development of metal hydride complexes that are easier to oxidize than the base present in solution would improve efficiency.[30] Ongoing efforts to develop new electrochemical activation methodologies will expand future opportunities for acceptorless C–H functionalization of substrates lacking directing groups.

Conflicts of interest

There are no conflicts to declare.

Acknowledgements

The synthesis and cyclic voltammetry were supported through funding from NSF Center for Enabling New Technologies through Catalysis (CENTC), CHE-1205189. Controlled potential electrolysis and thermal C–H activation studies were supported through the NSF Chemical Catalysis program under Grant No. CHE-1665135 and CHE-1665146.

Notes and references

1 J. A. Labinger and J. E. Bercaw, *Nature*, 2002, **417**, 507–514.
2 J. F. Hartwig, *J. Am. Chem. Soc.*, 2016, **138**, 2–24.
3 J. Choi, A. H. R. MacArthur, M. Brookhart and A. S. Goldman, *Chem. Rev.*, 2011, **111**, 1761–1779.
4 T. J. Hebden, K. I. Goldberg, D. M. Heinekey, X. Zhang, T. J. Emge, A. S. Goldman and K. Krogh-Jespersen, *Inorg. Chem.*, 2010, **49**, 1733–1742.
5 K. B. Renkema, Y. V Kissin and A. S. Goldman, *J. Am. Chem. Soc.*, 2003, **125**, 7770–7771.
6 M. Yan, Y. Kawamata and P. S. Baran, *Chem. Rev.*, 2017, **117**, 13230–13319.
7 M. D. Kärkäs, *Chem. Soc. Rev.*, 2018, **47**, 5786–5865.
8 N. Sauermann, T. H. Meyer, Y. Qiu and L. Ackermann, *ACS Catal.*, 2018, **8**, 7086–7103.
9 C. Ma, P. Fang and T. S. Mei, *ACS Catal.*, 2018, **8**, 7179–7189.
10 A. Jutand, *Chem. Rev.*, 2008, **108**, 2300–2347.

11 F. Novak, B. Speiser, H. A. Mohammad and H. A. Mayer, *Electrochim. Acta*, 2004, **49**, 3841–3853.
12 D. A. Laviska, PhD thesis, Rutgers University, 2013.
13 T. R. O'Toole, J. N. Younathan, B. P. Sullivan and T. J. Meyer, *Inorg. Chem.*, 1989, **28**, 3923–3926.
14 S. D. Pike, M. R. Crimmin and A. B. Chaplin, *Chem. Commun.*, 2017, **53**, 3615–3633.
15 V. M. Iluc, A. J. M. Miller, J. S. Anderson, M. J. Monreal, M. P. Mehn and G. L. Hillhouse, *J. Am. Chem. Soc.*, 2011, **133**, 13055–13063.
16 A. G. Walden, A. Kumar, N. Lease, A. S. Goldman and A. J. M. Miller, *Dalton Trans.*, 2016, **45**, 9766–9769.
17 O. B. Ryan, M. Tilset and V. D. Parker, *J. Am. Chem. Soc.*, 1990, **112**, 2618–2626.
18 J. D. Hackenberg, S. Kundu, T. J. Emge, K. Krogh-Jespersen and A. S. Goldman, *J. Am. Chem. Soc.*, 2014, **136**, 8891–8894.
19 G. P. Connor, N. Lease, A. Casuras, A. S. Goldman, P. L. Holland and J. M. Mayer, *Dalton Trans.*, 2017, **46**, 14325–14330.
20 B. Olgemoeller and W. Beck, *Inorg. Chem.*, 1983, **22**, 997–998.
21 A. M. Camp, M. R. Kita, J. Grajeda, P. S. White, D. A. Dickie and A. J. M. Miller, *Inorg. Chem.*, 2017, **56**, 11141–11150.
22 M. Brookhart, M. L. H. Green and G. Parkin, *Proc. Natl. Acad. Sci.*, 2007, **104**, 6908–6914.
23 S. A. Hauser, J. Emerson-King, S. Habershon and A. B. Chaplin, *Chem. Commun.*, 2017, **53**, 3634–3636.
24 E. Clot, M. Besora, F. Maseras, C. Mégret, O. Eisenstein, B. Oelckers and R. N. Perutz, *Chem. Commun.*, 2003, **98**, 490–491.
25 E. Clot, C. Mégret, O. Eisenstein and R. N. Perutz, *J. Am. Chem. Soc.*, 2009, **131**, 7817–7827.
26 M. E. Evans, C. L. Burke, S. Yaibuathes, E. Clot, O. Eisenstein and W. D. Jones, *J. Am. Chem. Soc.*, 2009, **131**, 13464–13473.
27 X. Zhang, M. Kanzelberger, T. J. Emge and A. S. Goldman, *J. Am. Chem. Soc.*, 2004, **126**, 13192–13193.
28 A. Casuras, PhD thesis, Rutgers University, 2019.
29 D. A. Ahlstrand, A. V. Polukeev, R. Marcos, M. S. G. Ahlquist and O. F. Wendt, *Chem.–Eur. J.*, 2017, **23**, 1748–1751.
30 C. R. Waidmann, A. J. M. Miller, C.-W. A. Ng, M. L. Scheuermann, T. R. Porter, T. A. Tronic and J. M. Mayer, *Energy Environ. Sci.*, 2012, **5**, 7771–7780.